J. Geogr. Sci. 2018, 28(3): 323-336
DOI: https://doi.org/10.1007/s11442-018-1475-z

Spatial and temporal variation of the urban impervious surface and its driving forces in the central city of Harbin

LI Miao[1], *ZANG Shuying[1], WU Changshan[2], NA Xiaodong[1]

1. School of Geographical Sciences, Harbin Normal University, Harbin 150025, China;
2. Department of Geography, University of Wisconsin–Milwaukee, PO Box 413, Milwaukee, WI 53201-0413, USA

Abstract: Associated with the rapid economic development of China, the level of urbanization is becoming a serious concern. Harbin, the capital city of Heilongjiang Province, China and one of the political, economic, cultural, and transportation centers of the northeastern region of China, has experienced rapid urbanization recently. To examine the spatial patterns of long-term urbanization and explore its driving forces, we employed the impervious surface fraction derived from remote sensing image as a primary indicator. Specifically, urban impervious surface information for the central city of Harbin in 1984, 1993, 2002, and 2010 was extracted from Landsat Thematic Mapper image using a Linear Spectral Mixture Analysis (LMSA). Then, the spatial and temporal variation characteristics and the driving factors of percent impervious surface area (ISA) changes were analyzed throughout this 26-year period (1984 to 2010). Analysis of results suggests that: (1) ISAs in the central city of Harbin constantly increased, particularly from 1993 to 2010, a rapid urbanization period; (2) the gravity center of impervious surface area in the central city was located in Nangang District in 1984, moving southeast from 1984 to 1993, northwest from 1993 to 2002, and continuing toward the southeast from 2002 to 2010; and (3) the urban growth of the central city can be characterized as edge-type growth.

Keywords: central city of Harbin; urban impervious surface; dynamic change; driving force

1 Introduction

Urban expansion, one of the basic characteristics of urbanization, is considered an important factor influencing the natural urban ecosystem. Urban expansion inevitably causes land cover changes, shown by the rapid conversion from natural cover to artificial cover (Kuang, 2012). Therefore, precise spatial and temporal dynamic information regarding urban land cover is required to understand the dynamics of the mechanism of the effect of urbanization

Received: 2017-01-31 **Accepted:** 2017-04-01
Foundation: Natural Science Foundation of Heilongjiang Province, No.QC2016050; National Natural Science Foundation of China, No.41571199, No.41601382, No.41771195
Author: Li Miao (1984–), PhD, specialized in land use/cover change and urban remote sensing.
E-mail: dkylimiao@163.com
***Corresponding author:** Zang Shuying (1963–), Professor, E-mail: zsy6311@163.com

within the regional ecosystem evolution. Land-Use and Land-Cover Change (LUCC) data is used for most research on urban expansion. However, the land cover changes brought about by urban expansions are generally shown by gradient features, rendering it impossible to use Land-Use and Land-Cover Change to effectively identify inner heterogeneous characteristics of the same land cover type. Changes in the impervious surface are the main indicators of urban expansion. Urban impervious surfaces refer to the artificial materials that water cannot penetrate to soil. For impervious surface, a continuous value of 0–1 is used to represent the percentage of impervious surface in each pixel. Impervious surfaces, a typical land cover constituent, can effectively describe the spatial gradient features of land cover changes (Ridd 1995; Li and Wu, 2016). It is a significant indicative factor for urban environmental quality and urban ecosystems, and its growth is closely related to driving factors such as urban development strategic targets and overall urban planning, significantly effecting the sound sustainable development of a city (Wang, 2013). Impervious surface produces a direct effect on regional vertical radiation balance through changes in surface albedo, emissivity, and surface roughness. This is caused by changes within the urban surface structure, thereby aggravating the surface sensible heat flux and heat island intensity, changing the regional climate, and affecting urban ecosystem service functions, particularly the thermal regulation function (Haashemi *et al*., 2016). Concurrently, urban impervious surfaces exhibit poor water storage capacity and obstruct air current transmission, resulting in substantial eco-environmental element effects, such as the urban land surface hydrological cycle, non-point source pollution, and biodiversity, thus becoming an important cause of urban eco-environmental changes. Yang and Liu (2005) and Yang (2006) have utilized the urban impervious surface to analyze the speed and spatial features of urban growth and have suggested that urban impervious surface information indicates urban expansion. Weng (2004) and Hao (2016) demonstrated that distribution of the urban impervious surface has an important relationship with the urban heat island effect. In addition to being used to measure the natural environment and ecological health, the urban impervious surface also reflects the urban inner structure, which is closely linked with urban social and humanistic conditions (Weng *et al*., 2009; Yuan and Bauer, 2007). Wu and Murray (2005, 2007) have utilized urban impervious surface information to estimate the detailed distribution information of residential population of a city. Yu and Wu (2004) demonstrated that urban impervious surface information can reflect quality of living and have used it to study urban population isolation. Research by Yu and Wu (2006) found that the urban impervious surface has certain effects on housing prices. Therefore, the extraction of urban impervious surface information has become a hot topic, with research on dynamic changes in the urban impervious surface being of great practical significance.

We chose the central city of Harbin as the study area to analyze the spatial and temporal patterns of impervious surface and the associated driving forces during a 26-year period (1984 to 2010). Further, these spatial and temporal patterns of impervious surface were examined through employing a boosted regression tree method with eight selected driving forces, including slope, aspect, DEM, distance to rivers, distance to expressways, distance to railways, distance to main roads, and distance to the city center. With the relationship between driving forces and impervious surface dynamics, this research may provide implications for urban planning policies.

2 Study area and data

2.1 Study area

Harbin city, located in the southwest of Heilongjiang Province, China, was selected as the study area. It is surrounded by the middle reaches of the Songhua River, between Xiao Hinggan Mountains and Zhangguangcai Ridge (see Figure 1). Harbin's geographical coordinates are approximately 125°42'–130°10'E and 44°04'–46°40'N, with a total geographic area of 53,100 km^2. It has an average annual temperature of 3.4℃, average annual evaporation of 1326 mm, average annual frost-free period of 130 days, and average annual rainfall of 500 mm. Harbin is the capital city of Heilongjiang Province and one of the political, economic, and cultural centers, and transport hubs in Northeast China. Harbin has been gradually developed into a synthetic city (Song and Gao, 2008), with the largest geographical area and second in terms of residential population within all provincial cities in China.

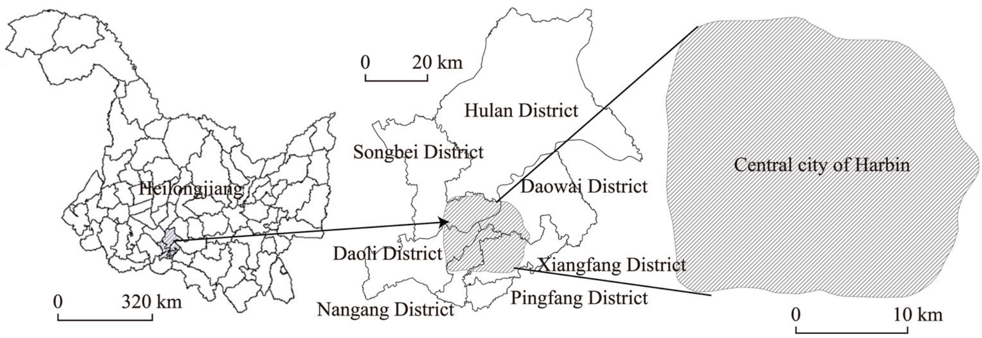

Figure 1 Location of the study area

2.2 Dataset

For this research, Landsat Thematic Mapper (TM) images and Digital Elevation Model (DEM) data were obtained from the United States Geological Survey. These imageries were re-projected to the Universal Transverse Mercator (UTM) coordinate system with a datum of the World Geodetic System 84 (WGS84). Statistical data were extracted from China City Statistical Yearbook and Harbin City Statistical Yearbook covering 1984, 1993, 2002 and 2010. The TM images on September 14, 1984; September 7, 1993; September 16, 2002; and September 22, 2010 were selected. The 2002 image was with a cloud coverage of 3%, but after cropping, the cloud coverage in the research area was 0%. For further analyses, bands 1–5 and 7 of the TM data with a spatial resolution of 30 m were selected.

2.3 Remote sensing data preprocessing

2.3.1 Geometric correction

For this research, the 2010 TM image, which has gone through precise geometric correction, was selected as the base map to correct other images. For georeferencing, the polynomial geometric correction module embedded in ERDAS Imagine 9.2 was utilized, with UTM as the coordinate system and WGS 84 as the datum to ensure the exact matching of sampling point positioning coordinates and remote sensing image projection coordinates (Mei, 2001; Markham, 1986). After the determination of projection parameters, 60 ground control points

(GCPs), including road intersections, building corners, and other well-defined objects, were selected through field work and careful examination of Google Earth high resolution aerial photos. With the georeference, the total root mean squared error (RMSE) was controlled within 0.5 pixel, indicating a satisfactory geometric positioning accuracy.

2.3.2 Radiometric correction

Radiometric calibration is a process in which the digital numbers (DNs) recorded by the sensor are converted to absolute radiance values (Liang, 2009; Liu *et al*., 2005) or to relative values relating to surface reflectance or surface temperature. In this research, a Landsat Calibration special module provided by ENVI 4.7 was employed for radiometric calibration, according to the following formula:

$$L_\lambda = LMIN_\lambda + \left(\frac{LMAX_\lambda - LMIN_\lambda}{QCALMAX - QCALMIN} \right) \left(QCAL - QCALMIN \right) \quad (1)$$

where $QCAL$ is the DN of the original quantization; $LMINX_\lambda$ is the radiance pixel value in the case of $QCAL = 0$; and $LMAX_\lambda$ is the radiance pixel value in the case of $QCAL$ = $QCALMAX$.

3 Methods

3.1 Linear Spectral Mixture Analysis (LSMA)

The pixels in remote sensing images are rarely pure pixels consisting of a single uniform land cover, but rather mixed pixels comprising several kinds of land covers. In spite of different spectral characteristics within different land covers, the pixels involved in sensing records only have a single spectral characteristic, i.e., the characteristics of several types of land covers are mixed. Therefore, the spectral characteristics of pixels in the image are not the spectral characteristics of a single land cover but are a mixed reflection of the spectral characteristics of several types of land covers (Tang and Xu, 2014). If a mixed pixel can be decomposed, and the percentage that its land cover type constituent occupies in the pixel can be obtained, misclassification problems caused by the attribution of the mixed pixel can be solved. This process is generally referred to as spectral mixture analysis (SMA). SMA can refine remote sensing classification from the pixel level to the sub-pixel level, thus providing a superior solution to the mixed pixel problem. SMA comes in a linear type and a nonlinear type, with many researchers proposing different impervious surface estimate methods based on SMA models. Linear SMA (LSMA) is widely used for the extraction of impervious surface data from remote sensing images with medium and coarse resolution. A linear spectral mixture model is defined as the reflectivity of a pixel at a certain band being a linear combination of the reflectivity of several different endmembers, with the percentage they occupy in the pixel area as a weight coefficient (Wu *et al*., 2006), as shown in the following formula:

$$R_i = \sum_{k=1}^{n} f_k R_{ik} + \varepsilon_i \left(\sum_{k=1}^{n} f_k = 1, 0 \leqslant f_k \leqslant 1 \right) \quad (2)$$

where R_i is the reflectivity of Band i of a mixed pixel, containing one or more endmember components; k represents a particular endmember, and n is the number of end members; f_k is the percentage of endmember k inside the pixel; R_{ik} is the reflectivity of endmember k at band i; and ε_i is the fitting error of the model at band i.

3.1.1 Endmember selection

A scatter diagram shows the distribution of the vector in the reflectivity space that is made up of the reflectivity values in the same pixel position of different bands. For this research, endmembers were selected through analyzing the N-dimensional feature space interactions of the first three principal components obtained through principal component analysis (PCA) transformation. Figure 2 depicts the space scatter diagram of the first three component end-members after PCA transformation of four images. Endmembers are selected through pure pixels of each category and are generally distributed at the top point of a triangular feature space; the closer to the edge, the higher the purity. Endmember include high albedo, low albedo, soil, and vegetation.

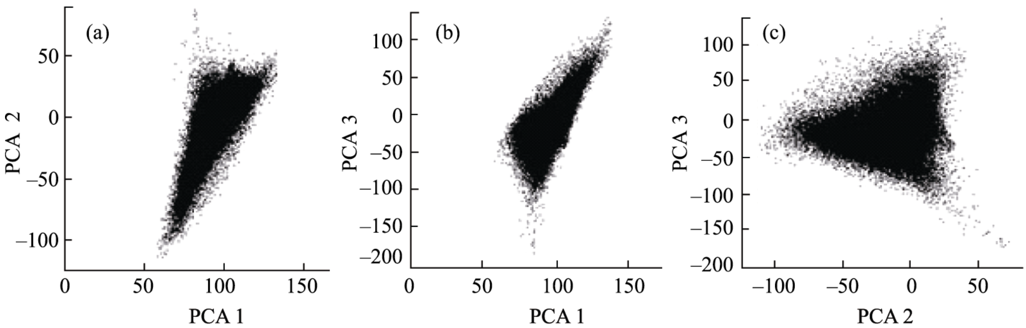

Figure 2 Feature space representation of the first three PCA components

3.1.2 Accuracy assessment

Mean absolute error (MAE) and root-mean-square error (RMSE) were used to evaluate the accuracy. MAE reflects the practical situation of the predicted value error as an absolute value employed for dispersion, avoiding the offset of positive and negative values, and the RMSE is capable of evaluating the deviation between the observed value and true value.

$$MAE = \frac{1}{n}\sum_{i=1}^{n}\left|f_i - y_i\right| \tag{3}$$

$$EMSE = \sqrt{\frac{1}{n}\sum_{i=1}^{n}(f_i - y_i)^2} \tag{4}$$

where f_i is the estimated percentage of endmember i within a sample; y_i is the measured percentage of endmember i for the sample, and n is the total number of samples.

For the selection of samples, we used a random sampling strategy to choose 200 samples from the original image. A sample size of 3×3 pixel, which could reduce the effect of geometric error, was employed. The actual proportion of impervious surface in the 3×3 pixel was calculated by visual interpretation and digitization. The proportion of the impervious surface derived from LSMA was then calculated. Finally, RMSE and MAE were calculated to be 0.19 and 0.14, respectively, thus indicating the applicability of present result.

3.2 Boosted regression tree

The boosted regression tree（BRT）is an ensemble learning method based on the Classification and Regression Tree (CART) algorithm. This method produces a multiple regression tree through random selection and a self-learning method that is able to improve the model stability and prediction accuracy (Li *et al*., 2014; Elith *et al*., 2008). The BRT algorithm is an optimization technology involving the minimized loss function's prediction of the residual value of the previous tree through repeated fitting of the new tree. BRT involves random selection of a certain quantity of data a given number of times in the operation process to analyze the effect of independent variables on dependent variables, and the remaining data is used to test the fitting result. The use of BRT within urban expansion research can help obtain not only the relative effect of each driving factor but also the mechanism of the relationship between relative effect and the changes in each driving factor, thereby obtaining accurate and intuitive results (Freund and Schapire, 1997).

4 Results and discussion

4.1 Impervious surface expansion analysis

The distributions of impervious surfaces from 1984 to 2010 (see Figure 3) illustrate obvious spatial variations over this period. In 1984, the impervious surface in Harbin was mainly concentrated within the city center. In spite of a small geographical area, there were a number of impervious surface areas with high percent coverage. In 1993, the area of impervious surface expanded. In 2002, the area of impervious surface did not expand significantly when compared with the area in 1993, but the scope of impervious surface expanded a lot in terms of scope, with impervious surface distributed north of the Songhua River. In 2010, the impervious surface significantly expanded to the north of the Songhua River, with the distribution of impervious surface patches with high coverage found.

From 1984 to 1993, the area of the impervious surface increased from 48.51 to 57.1 km^2, with an increased rate of 0.95 km^2 per year. From 1993 to 2002, the area of the urban impervious surface increased from 57.1 to 72.85 km^2, with an increased rate of 1.75 km^2 per year. In 2010, the area of impervious surface increased to 125.04 km^2. The increased area of impervious surface during the 8-year period from 2002 to 2010 was more than three times that during the period from 1993 to 2002. The increased area of impervious surface during the 8-year period from 2002 to 2010 doubled with respect to that during the period from 1984 to 2002, indicating rapid development within the city during the period 2002–2010.

4.2 Shift of the gravity center of the impervious surface in the central city

In this study, the calculation of the gravity center shift of the urban impervious surface in the city center is not based on a simple gravity center calculation but on dividing the percentage of impervious surface in the pixel into 10 grades from 0.1 to 1 at 0.1 intervals. Then, each grade is given a corresponding weight, based on which the calculation is conducted, yielding the gravity center shift of the urban impervious surface in the Harbin city center from 1984 to 2010. From 1984 to 2010, the gravity center of the urban impervious surface in the city

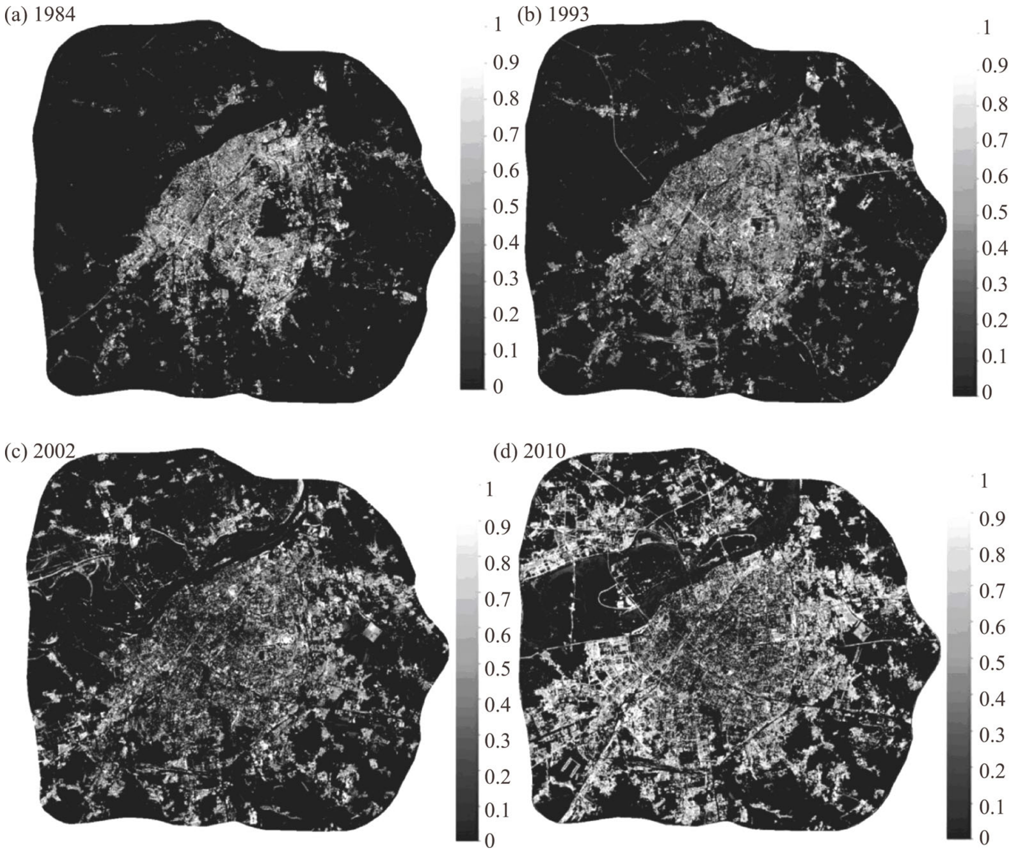

Figure 3 Distribution of impervious surfaces in Harbin central city (1984–2010) (a. 1984; b. 1993; c. 2002; d. 2010)

center was distributed in the Nangang District, but moved 346.26 m towards the southeast during 1984–1993, which is consistent with the results of the impervious surface pattern analysis above, because the impervious surface mainly spread towards the south from 1984 to 1993. From 1993 to 2002, the gravity center of the urban impervious surface in the central city moved 685.68 m towards the northwest, with the movement direction being the opposite of that from 1984 to 1993 and the movement distance being nearly twice that from 1984 to 1993. From 2002 to 2010, the impervious surface in the central city continued to move 877.51 m towards the northwest.

4.3 Analysis of the driving force for impervious surface changes

The spatial characteristics of land cover can be effectively described by impervious surface. The growth level of the impervious surface area is closely related to the urban population, urban economic development, overall urban planning, and other driving factors. In this study, population, economic, and planning factors were selected as the external drivers of variation in the urban impervious surface area. Internal driving factors included slope, aspect, DEM, distance from the river, distance from the highway, distance from the railway, distance from the main road, and distance from the urban area. These external and internal driving factors were selected for analysis of the driving force behind variation in the urban impervious surface.

4.3.1 External factors affecting impervious surface area variation

The non-agricultural population is an important factor reflecting the urbanization level of a region. Because variation in the non-agricultural population inevitably leads to expansion of the urban area, the non-agricultural population was selected as the demographic factor index in this study. With the development of the socialist market economy, the regulating function of the market economic system plays a very important role in the exploitation and utilization of land resources. Gross Domestic Product (GDP) is often recognized as the best indicator of the state of the country's economy. Harbin is the former northeastern industrial base, and the proportion of its secondary industry in GDP is also an important factor in urban land expansion. In recent years, Harbin has undergone industrial restructuring, and the proportion of its tertiary industry in GDP has also become a significant factor. Meanwhile, the development of the urban construction industry is directly reflected by its increased gross output. During this period of rapid economic growth, personal income was also on the rise. Brueckner (2000) suggested that the increase of personal income is one of the main driving factors of urban spatial expansion. Because of their effects on urban expansion, population, GDP, GDP of the secondary and tertiary industries, average wage, and GDP of the construction industry were selected to analyze the driving forces of the variation in the urban impervious surface area (see Table 1).

Table 1 Driving factors and indices

Driving factors	Indices
Demographic factor	X_1 non-agricultural population
Economic factor	X_2 GDP X_3 total output of the secondary and tertiary industries X_4 the average wage X_4 GDP of the construction industry

(1) The population factor

In 1984, the non-agricultural population of Harbin was 2.59 million, with the urban population increasing to 4.72 million in 2010, a factor of 1.82 over 26 years. In this study, regression analysis was carried out for the non-agricultural population and the impervious surface area, as shown in Figure 4. The x-axis represents the impervious area, and the y-axis represents the non-agricultural population. The goodness of fit of a second order trend line is 0.967, indicating a high correlation of population growth to impervious surface area. Because of the population's production and living needs, a large amount of construction land is required to meet the needs of the spatial expansion. An increasing population requires additional houses, roads, factories, schools, and shopping malls, as well as supporting facilities. Furthermore, with improved living standards, people in pursuit of material goods will also pursue spiritual improvement, such that the number of tourism and entertainment

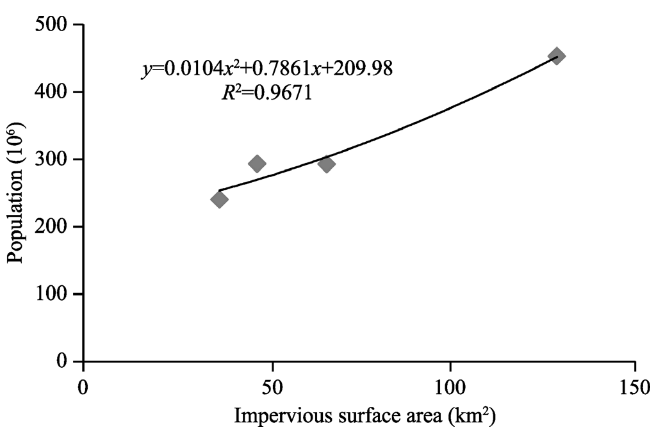

Figure 4 Non-agricultural population as a function of impervious surface area

will also increase, leading to additional development and a corresponding increase of the impervious surface area.

(2) The economic factors

In this study, regression analysis was carried out for the impervious surface area, GDP, GDP of the second and tertiary industries, average wage, and GDP of the construction industry, as shown in Figure 5. The x-axis represents the impervious area and the y-axis in each of the four graphs represents GDP, GDP of the second and tertiary industries, average wage, and GDP of the construction industry, respectively. The correlations measured 0.998, 0.998, 0.999, and 1.0, respectively. During the 15 years spanning the 9th–11th Five-Year Plans, the economic level of Harbin improved significantly. In 1984, the GDP of Harbin was 6.88 billion yuan, and increased to 366.99 billion yuan in 2010, a factor of 53.27 over 26 years. Similarly, the GDP of the secondary and tertiary industries increased from 5.26 billion yuan in 1984 to 325.2 billion yuan in 2010, and the proportion of the secondary and tertiary industries increased from 76.45% to 88.7%, respectively, over the same time period. The development of the secondary industry not only increased the industrial land area but also led to a large number of people moving into the city, causing the urban housing land area to increase. Furthermore, the development of the tertiary industry also caused the urban impervious surface area to increase. In Harbin, the average wage in 1984 was 996 yuan and 32,397 yuan in 2010, an increase by a factor of 32.53. With improvement in living standards, more people buy houses, expanding the real estate industry and subsequently causing the urban impervious surface area to increase.

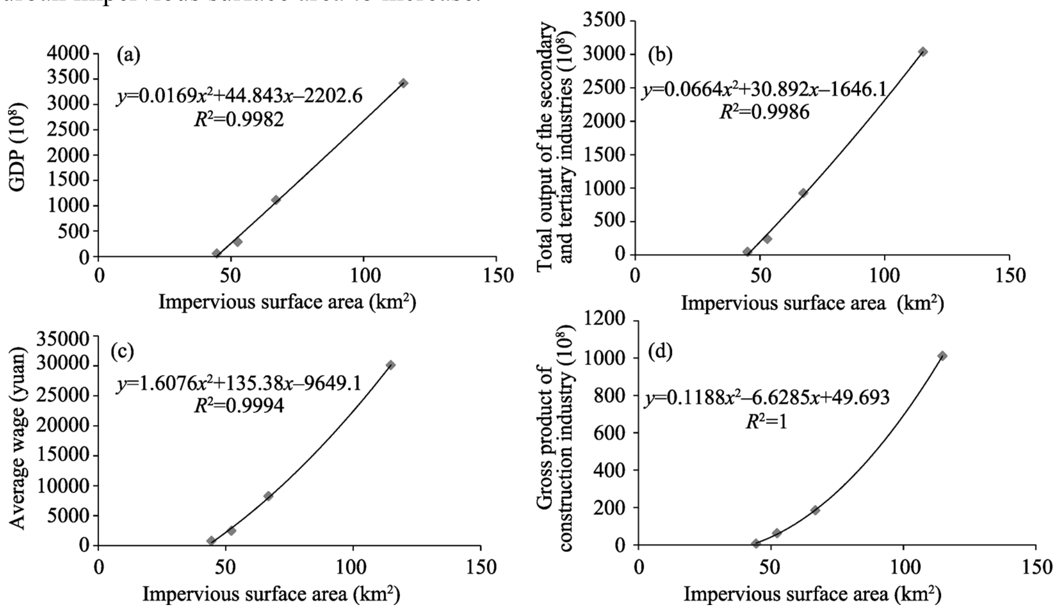

Figure 5 Function of impervious surface area (a. GDP; b. total output of the secondary and tertiary industries; c. average wage; d. gross product of construction)

(3) The planning factors

The ‘Decision on Economic Restructuring’ adopted in 1984 suggested that the reformation focus was shifted from rural areas to urban areas. During the 10th Five-Year Plan (2001–2005), the process of urban planning approval in Harbin was reformed. During these five years, 5623 construction projects of various types were approved, adding floor area of 41.27 km^2. These projects included more than 80 shantytown renovation projects and more than 1500 urban infrastructure construction projects. During the 10th Five-Year Plan (2001–2005), the developed area increased from 211 km^2 to 318 km^2. During the 11th Five-Year Plan (2006–2010), the municipal government proposed an increase in the residential land area, as well as public and municipal facilities, which led to an increase in the urban impervious surface area.

4.3.2 Internal factors affecting impervious surface area variation

The dependent variable in this study was the increase in the impervious surface in the city center from 1984–2010. Through the different operations based on the urban impervious surface within the city center during 1984 and the urban impervious surface diagram in 1984, the magnitude of change in the urban impervious surface in the city center from 1984 to 2010 is obtained. Zero means that in 1984 and 2010 no urban impervious surfaces were involved, indicating no new buildings in this area. A number greater than 0 indicates no impervious surface in 1984 and impervious surface in 2010, or that the percentage of impervious surfaces in 2010 is greater than that in 1984, showing an increase in the number of buildings in this area. A one is assigned to anything greater than 0, and this change value depicts a dependent variable. Eight factors are selected: slope, aspect, DEM, distance from the river, distance from the highway, distance from the railway, distance from the main road, and distance from the urban area in 1984. The eight driving factors are as shown in Figure 6. DEM is between 98 m and 199 m, with the northern DEM lower than the southern DEM in general. The distance from the main urban area in 1984 is 0–11,433.9 m, with a uniform distance from the central city as a whole. The northwestern section is a bit longer than that in

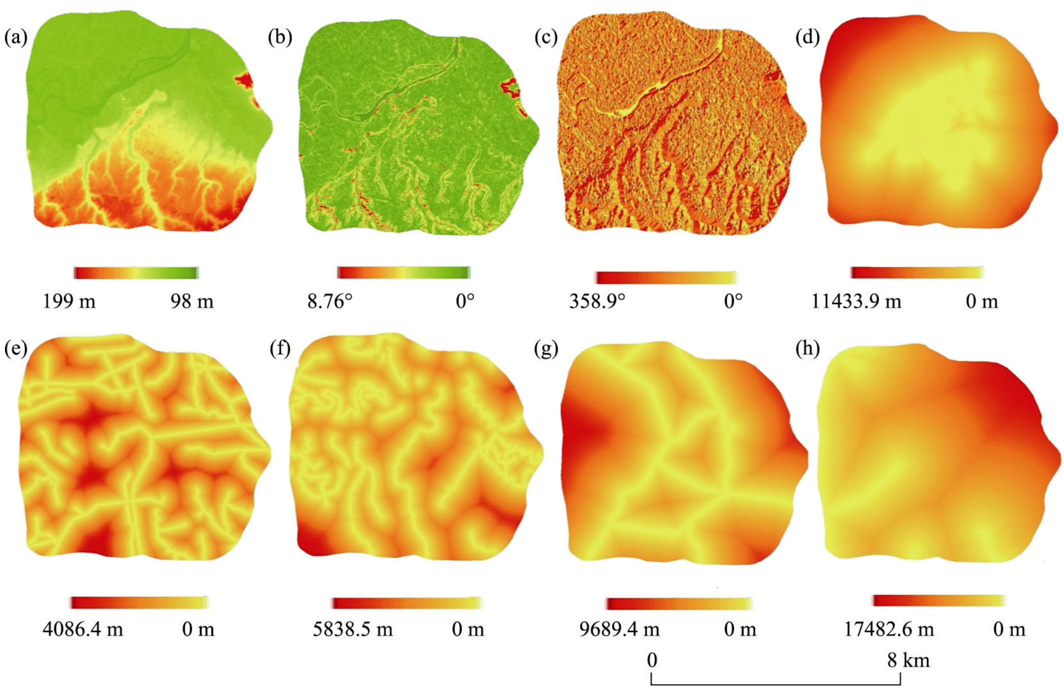

Figure 6 Driving factors (a. DEM; b. slope; c. aspect; d. distance from city center of 1984; e. distance from

main road; f. distance from river; g. distance from railway; h. distance from highway)

other parts. Main roads and railways are distributed in various directions in the central city owing to the prevalence of highways; the distances are distributed in a strip shape. The eight factors are obtained through the Spatial Analyst Tool module in ArcGIS, with 10,000 sample points randomly generated. Then the attribute values within the points for each figure layer correspondence are exported, and finally the data is imported into the software R for the BRT analysis. The Elith program is utilized for the BRT analysis, with the learning rate set to 0.005. Fifty percent of the data is extracted for analysis each time, and the remaining 50% of the data was used as training, with cross validation conducted five times. The BRT operation is conducted in R. The relative operating characteristic (ROC) value is 0.923, indicating the results is significant.

Through the BRT analysis, the effect of each factor on the changes in the impervious surface in the Harbin city center is analyzed; the factor that has the greatest effect is the distance from the urban area, with its contribution rate being the highest, 29%. The contribution rates of the other driving factors in order from the largest to the smallest are as follows: DEM (13.4%), distance from the highway (12.4%), distance from the railway (12.2%), distance from the river (10.3%), distance from the main road (9.9%), slope (6.8%), and aspect (6%).

The analysis shows that neighborhood factors have a great effect on the urban impervious surface, with the relative effect of five neighborhood factors on the urban impervious surface ranking 1st, 3rd, 4th, 5th, and 6th among all factors, with their total effect reaching up to 73.8%. DEM also plays a significant role in the increase of the impervious surface of the city center, with a relative effect of 13.4%, ranking second among the eight factors.

Figure 7 shows the effect change curves of the relative effects of driving factors, and these curves show the changes with the values taken for the driving factors and the changes in their effects on the urban impervious surface. When the relative effect value is greater than 0, the effect of the driving factors on the increase in the urban impervious surface is positive. When the relative effect value is less than 0, the effect of the driving factors on the urban impervious surface is negative. When the value is 0, there is no relationship. The distance to the urban area reflects the importance of geographical location. The Harbin city center provides goods to the surrounding areas, and the influence of the city center decreases with increasing distance. The relative effect of the distance from the urban area in 1984 demonstrates that the effect decreases with an increase in distance from the city center. When the distance from the urban area is within 4300 m, the effect of the distance to the urban area on the urban impervious surface shows a positive correlation: the closer to the urban area, the greater the effect. When the distance is larger than 4300 m, the effect is negative, such that the distance has a restrictive effect on the urban impervious surface. When the distance is greater than 10,000 m, it is beyond the urban radiation effect scope, and the distance to the urban area has almost no effect on the urban impervious surface. Harbin is a flat terrain plain area, with a low altitude. When the DEM is between 120 m and 165 m, the relative effect is positive, which indicates that the altitude in this area is suitable for urban development. Because of the presence of many rivers in Harbin, the altitude has a restrictive effect on urban expansion. Highways, railways, and main roads are the main transport carriers of traffic flows and logistics in modern cities, which is of great significance for urban spatial expansion, having a direct effect on the urban expansion direction. When there is a distance of 5600 m from the railway and 1000 m from the main road, the relative effect is positive, indicating social and economic development can be created in this area, thereby contributing to the urban expansion along the railway or the road.

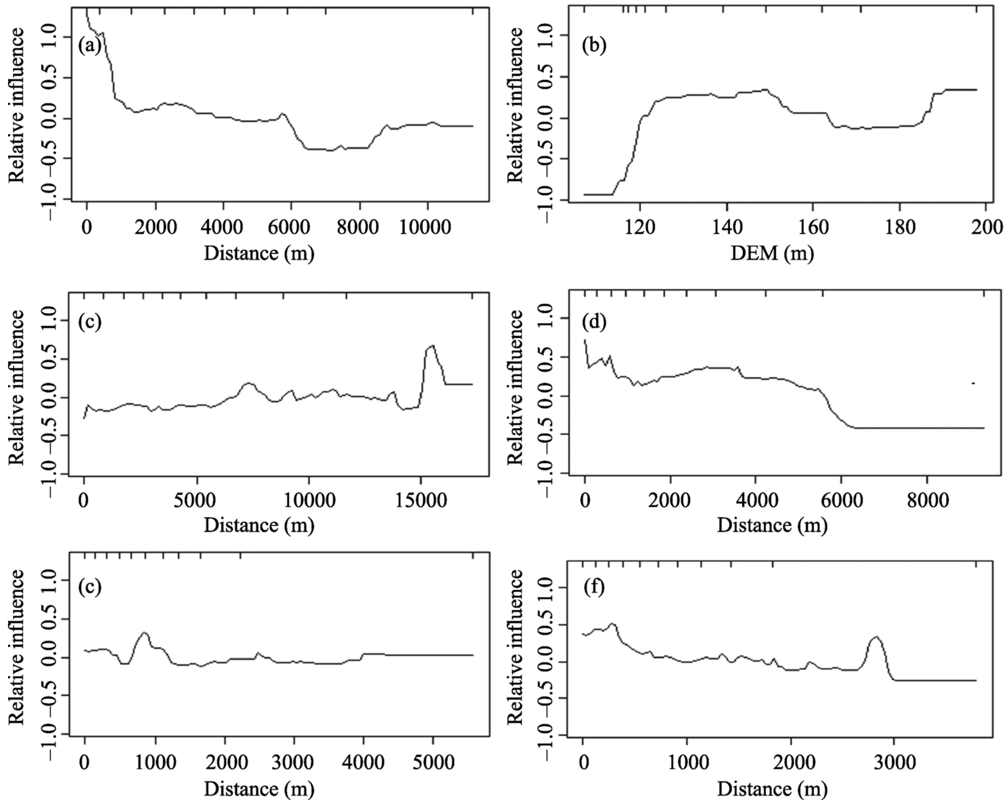

Figure 7 Relative influence on the change of impervious surface in the central city
(a. distance from the city center of 1984; b. DEM; c. distance from highway; d. distance from railway; e. distance from river; f. distance from main road)

5 Conclusions and limitations

By using the Landsat TM in 1984, 1993, 2002, and 2010 as a reference for the central city of Harbin, the urban impervious surface was extracted using the linear spectral mixture analysis method. The spatial and temporal variation characteristics of the urban impervious surface in the city center were analyzed, and the factors influencing the expansion of the urban impervious surface in the city center during a 26-year period (1984 to 2010) were further analyzed, with specific conclusions as follows:

(1) From 1984 to 2010, the impervious surface coverage of Harbin city continued to increase, particularly from 2002 to 2010 during which rapid increase occurred. The city center has constantly spread.

(2) From 1984 to 2010, the gravity center of the urban impervious surface in Harbin city center was distributed throughout Nangang District but moved to the southeast from 1984 to 1993, to the northwest from 1993 to 2002, and continued to move towards the southeast

from 2002 to 2010. This is due to the rapid development of Songbei District under the development strategy “Southern Leap, Northern Expansion, Central Revitalization, and County Strengthening,” showing a close link between urban expansion and policies of development planning.

(3) The driving force of the urban expansion was analyzed, and regression analysis was carried out in order to quantify the correlation between population and economic changes and impervious surface area changes. Additionally, the influence of planning policies on the increase of the urban impervious surface was analyzed. It can be seen that population, economic factors, and planning policies all play a positive role in increasing the impervious surface area.

(4) The relative effect of each driving factor on the expansion of the city center indicates that the expansion is mainly shown by edge-type growth. In other words, the closer to a city edge an area is, the more easily the area is developed into a city. The time scale in this study was very short, only 26 years, and over such a short time scale, natural factors have little effect on urban expansion.

(5) It has been difficult to account for the spatialization of socio-economic factors, which affects the analysis of driving factors to a certain degree. This study involves qualitative analysis of economic factors, with no good solutions to this problem presented. Efforts will be increased to make improvements in future research.

References

China City Statistical Yearbook. http://www.chinayearbook.com/yearbook. Accessed on 2013-03-01.

Elith J, Leathwick J R, Hastie T, 2008. A working guide to boosted regression trees. *Journal of Animal Ecology*, 77(4): 802–813.

Feng D J, Li Yongshu, Deng F, 2004. Detecting change information automatically by method of wavelet coefficient difference. *Remote Sensing Information*, (2): 13–15.

Freund Y, Schapire R E, 1995. A decision-theoretic generalization of on-line learning and an application to boosting. In: European Conference on Computational Learning Theory. Springer-Verlag: 119–139.

Hao P, Niu Z, Zhan Y *et al*., 2015. Spatiotemporal changes of urban impervious surface area and land surface temperature in Beijing from 1990 to 2014. *Giscience & Remote Sensing*, 53(1): 1–22.

Harbin City Statistical Yearbook. http://www.chinayearbook.com/yearbook. Accessed on 2013-03-01.

Kuan W H, 2012. Evaluating impervious surface growth and its impacts on water environment in Beijing-Tianjin-Tangshan Metropolitan Area. *Journal of Geographical Sciences*, 22(3): 153–165.

Li C L, Liu M, Hu Y M *et al*., 2014. Driving forces analysis of urban expansion based on boosted regression trees and logistic regression. *Acta Ecologica Sinica*, 34(3): 727–737.(in Chinese)

Li W L, Wu C S, 2016. A geostatistical temporal mixture analysis approach to address endmember variability for estimating regional impervious surface distributions. *Giscience & Remote Sensin*g, 53(1): 102–121.

Liang S L, 2009. Quantitative Remote Sensing. Beijing: Science Press, 14–16. (in Chinese)

Liu Z, Wang Y, Peng J *et al*., 2011. Using ISA to analyze the spatial pattern of urban land cover change: A case study in Shenzhen. *Acta Geographica Sinica*, 66(7): 961–971.(in Chinese)

Markham B L, 1986. Landsat MSS and TM Post-Calibration Dynamic Ranges, Exoatmospheric Reflectances and At-Satellite Temperatures. Landsat Technical Notes, 3–8.

Mei X A, Peng W L, Qing Q M *et al*., 2001. Introduction to Remote Sensing. Beijing: Higher Education Press. (in Chinese)

Song G, Gao N, 2008. Economic benefit analysis of urban land utilization based on DEA method: A case of

Harbin City. *Scientia Geographica Sinica*, 28(2): 185–188. (in Chinese)

Tang F, Xu Q, 2014. Comparison of performances in retrieving impervious surface between hyperspectral (Hyperion) and multispectral (TM/ETM+) images. *Spectroscopy and Spectral Analysi*s, 4: 1075–1080.

Wang D, 2013. Study on urban growth based on information extraction of impervious surface from remote sensing imagery: A case study on urban built-up area of Lanzhou City [D]. Lanzhou: Lanzhou University. (in Chinese)

Weeks J R, 2005. Measuring temporal compositions of urban morphology through spectral mixture analysis: Toward a soft approach to change analysis in crowded cities. *International Journal of Remote Sensin*g, 26(4): 699–718.

Weng Q, Lu D, Schubring J, 2004. Estimation of land surface temperature–vegetation abundance relationship for urban heat island studies. *Remote Sensing of Environment*, 89(4): 467–483.

Weng Q H, Hu X F, Liu H, 2009. Estimating impervious surfaces using linear spectral mixture analysis with multitemporal ASTER images. *International Journal of Remote Sensing*, 30(18): 4807–4830.

Wu C, Murray A T, 2005. A cokriging method for estimating population density in urban areas. *Computers Environment & Urban Systems*, 29(5): 558–579.

Wu C, Murray A T, 2007. Population estimation using landsat enhanced thematic mapper imagery. *Geographical Analysis*, 39(1): 26–43.

Wu C Q, Wang Q, Yang Z F, 2006. Cloud-moving of water RS image based on mixed pixel model. *Journal of Remote Sensing*, 10(2): 176–183.

Yang X, 2006. Estimating landscape imperviousness index from satellite imagery. *IEEE Geoscience and Remote Sensing Letters*, 3: 6–9.

Yang X, Liu Z, 2005. Use of satellite-derived landscape imperviousness index to characterize urban spatial growth. *Computers*, *Environment and Urban System*, 29: 524–540.

Yu D L, Wu C S, 2004. Understanding population segregation from Landsat ETM+ imagery: A geographically weighted regression approach. *Giscience & Remote Sensing*, 41(3): 187–206.

Yu D L, Wu C S, 2006. Incorporating remote sensing information in modeling house values. *Photogrammetric Engineering & Remote Sensing*, 72(2): 129–138.

Yuan F, Bauer M E, 2007. Comparison of impervious surface area and normalized difference vegetation index as indicators of surface urban heat island effects in Landsat imagery. *Remote Sensing of Environment*, 106(3): 375–386.